12-2010

SOLID TARGET SYSTEM FOR USE ON AN 11 MeV CYCLOTRON

Andrew Carl Williamson
awilli13@utk.edu

To the Graduate Council:

I am submitting herewith a thesis written by Andrew Carl Williamson entitled "SOLID TARGET SYSTEM FOR USE ON AN 11 MeV CYCLOTRON." I have examined the final electronic copy of this thesis for form and content and recommend that it be accepted in partial fulfillment of the requirements for the degree of Master of Science, with a major in Mechanical Engineering.

William R. Hamel, Major Professor

We have read this thesis and recommend its acceptance:

Kivanc Ekici, G.V. Smith

Accepted for the Council:
Carolyn R. Hodges

Vice Provost and Dean of the Graduate School

(Original signatures are on file with official student records.)

To the Graduate Council:

I am submitting herewith a thesis written by Andrew Carl Williamson entitled “Solid Target System for use on an 11 MeV Cyclotron.” I have examined the final electronic copy of this thesis for form and content and recommend that it be accepted in partial fulfillment of the requirements for the degree of Master of Science, with a major in Mechanical Engineering.

William Hamel , Major Professor

We have read this thesis
and recommend its acceptance:

G.V. Smith

Kivanc Ekici

Accepted for the Council:

Carolyn R. Hodges
Vice Provost and Dean of the Graduate School

(Original signatures are on file with official student records.)

SOLID TARGET SYSTEM FOR USE

ON AN 11 MeV CYCLOTRON

A Thesis Presented for

The Master of Science

Degree

The University of Tennessee, Knoxville

Andrew Carl Williamson
December 2010

DEDICATION

To my family for all of their support.

ACKNOWLEDGEMENTS

I would like to thank my academic advisors
Dr. Bill Hamel, Dr. G.V. Smith and Dr. Kivanc Ekici
for their guidance and support.

ABSTRACT

Molecular imaging is becoming an important contributor to the development of personalized medicine. Positron Emission Tomography (PET) is a technology that enables molecular imaging by allowing a physician to detect and map the location of various physiological processes. The purpose of this work is to design, fabricate and test a mechanism that would make the production of the PET isotope, copper-64 practical for both researchers and commercial suppliers. In order to have the maximum usefulness, the design needs to fit and operate within several constraints. A one dimensional thermal analysis indicated that operation of the system under existing cooling conditions would be a reasonable solution. Based on the design specifications, a detailed design was completed and fabricated. The design was functionally and operationally tested with the performance meeting expectations. The design was utilized to produce copper-64 isotope with a typical one hour bombardment producing 30 mCi of isotope. The design could be optimized if future isotope demand exceeded current production capacity or if research required the production of other radioisotopes with varying thermal characteristics.

Table of Contents

List of Figures

List of Tables

1. Introduction

1.1 Molecular Imaging and PET

Personalized medicine is the use of new methods of molecular analysis to better manage a patient's disease or predisposition toward a disease. It aims to achieve optimal medical outcomes by helping physicians and patients choose the disease management approach likely to work best in the context of the patient's unique genetic and environmental profile [1]. Typical medical imaging techniques, such as CT scans and MRI, show the structure of the body being imaged. To diagnose a problem or disease it is also important to know what is taking place in that structure physiologically. Since all tissues operate on a chemical basis, knowing what chemical processes are occurring in the imaged tissue can provide information as to whether the tissue is diseased [2].

Molecular imaging is defined as the *in vivo* characterization and measurement of biologic processes at the cellular and molecular level. Molecular imaging is a key modality enabling the move to personalized tailored treatments. For example, molecular testing is being used to identify those breast cancer and colon cancer patients likely to benefit from new treatments [1].

Positron Emission Tomography (PET) is a type of molecular imaging where an unstable radioisotope from a radiopharmaceutical or biomarker emits a positron, which looses energy through collisions with surrounding atoms and molecules. The positron then combines with an electron and annihilates producing a pair of 511 keV photons, emitted

roughly 180 degrees apart. By monitoring the location of decay events with a ring of scintillating crystals, the location of the biomarker that is consumed in a body's biochemical process can be determined and imaged [2].

In recent years, PET has become a major diagnostic tool in determining the occurrence or stages of cancer because it shows on a fundamental level what is taking place within tissues. A major issue with commercial use of PET is that the short half lives of radioisotopes normally used for these studies generally requires they be made on-site. A common method of generating radioisotopes used in PET scans is through the use of cyclotrons. Cyclotrons accelerate a beam of particles in a circular path, increasing their energy until the beam is deposited onto a target containing the element to be transmuted into the desired radioisotope [3]. The costs associated with purchasing and maintaining a cyclotron creates barriers to PET adoption [2]. Most of the PET patient doses produced in the United States are produced by large commercial interests.

Research utilizing PET isotopes is sometimes limited by the radioisotope availability. Copper-64 is an example of a promising PET isotope which suffers from lack of commercial interest because it usually requires a dedicated target system [4]. This means a commercial producer would lose the ability to produce other isotopes on their cyclotron.

The 12.7-hour half-life of copper-64 provides the flexibility to image both smaller molecules and larger, slower clearing proteins. In a practical sense, the radionuclide can be easily shipped for PET imaging studies at sites remote to the production facility. Due to the versatility of copper-64, there has been an abundance of novel research in this

area, primarily in the area of PET imaging, but also for the targeted radiotherapy of cancer [4]. The most researched clinical application is for hypoxia detection in tumors [1]. Hypoxic tumors do not use oxygen and are thus not as sensitive to traditional chemotherapy. Compounds labeled with copper-64 are preferentially taken up by hypoxic cells compared to normoxic cells with the extent of retention in tissue being inversely related to the state of tissue oxygenation. This effect allows the quantification of tissue hypoxia by positron emission tomography. Biomarkers labeled with copper-64 radioisotope offer the potential to identify hypoxic tumors and provide the information necessary to modify treatment.

1.2 Purpose

The purpose of this work is to design, fabricate and test a mechanism that would make the production of copper-64 practical and appealing to both researchers and commercial suppliers. Specifically, the work is to design a solid target and handling system which would function on an existing commercial target platform that will maintain the ability to produce standard radioisotopes as well as copper-64. An optimized, efficient system that would allow a commercial supplier to offer standard liquid and gas target products along with solid target products would be beneficial to the development of PET.

1.3 Synopsis of Chapters

Chapters 1 and 2 provide introductory material and establish the purpose and applicability of the work. Chapter 3 details the design elements that were considered during the work. Areas of focus such as scope, basic concepts, materials, thermal and mechanical considerations are discussed. Chapter 4 establishes the operating

parameters and methodology for the design. Chapter 5 reviews the testing protocols and results for bench top, cyclotron and field testing. Chapter 6 offers summary and conclusions along with recommended future work.

2. Background

PET has been used in large scale clinical practice for the last 10 years. Numerous PET isotopes are commercially available on a daily on-demand basis. There are approximately 120 commercial cyclotrons in the United States and an additional 250 world wide dedicated to the production of PET isotopes. The most widely used PET isotopes are list in Table 1 [2].

Table 1 : Common PET Isotopes

Product	Target Material	Target Type	1/2Life (min)	Reaction
F-18	O-18	Liquid	110	O18(p,n)F18
C-11	N2 gas +2.5%O2	Gas	20	N14(p,alpha)C11
N-13	Sterile water + 5mmol EtOH	Liquid	10	O16(p,alpha)N13
O-15	(N15)N2+2.5%O2	Gas	2	N15(p,n)O15

All of these isotopes are produced from liquid or gas targets and they can be produced in adequate quantities from cyclotrons with proton energies above 7 MeV. In contrast, copper-64 is produced from a solid target material [5]. Generally, solid target reactions require energies at or above 11 MeV in order to produce quantities sufficient for commercial production.

Copper-64 is produced by the bombardment of nickel -64 with energetic protons. The production of copper-64 via energetic proton bombardment on a cyclotron was validated with low current irradiations and the feasibility of copper-64 production by this method was demonstrated by Szelecsenyi [6].

The handling and cooling requirements of solid targets differ from liquid and gas targets. The target material must be handled by a mechanical process as opposed to flow of a liquid or gas. Additional components for cooling and complexity of operation required to enable a solid target system make them less attractive to commercial suppliers.

3. Design

3.1. Scope

The scope of the design is to provide a target system which can be used to produce isotopes from solid targets and can be retrofitted onto an existing cyclotron without losing the ability to produce isotopes from liquid or gas targets. If successful, this will make the potential install base of cyclotrons immediately available for upgrade to the solid target option. To minimize the impact on standard production, the new design deployment should be capable of being installed in a relatively short time period.

The new solid target system must allow the use of all standard liquid and gas targets. If this were not the case, researchers might be unwilling to lose access to all liquid and gas produced isotopes in exchange for the somewhat limited production of copper-64. The solid target system must also operate within the existing envelope for space, control, and cooling systems.

From a performance standpoint, the system must be capable of producing useful quantities of the copper-64 isotope from cyclotrons that produce protons with energy of 11 MeV. For most research applications, this means use of 1-2 mCi for pre-clinical animal imaging and 10-20 mCi for clinical applications at injection. Therefore, when radioactive decay and chemical processing time are taken into account, the quantity from the target should be in excess of 30 mCi.

Another important consideration is that the design must limit the radiation exposure of personnel when loading or unloading the target with as much of the operation as possible being automatically and remotely controlled.

3.2. Concepts

3.2.1. Nuclear Reactions

The three most common types of targets used to produce PET radioisotopes are liquid and gas and solid. In addition, the most common PET radioisotope is fluorine-18, of which approximately 1.5 million doses are produced annually in the United States. The primary use of fluorine-18 is in oncology for treatment monitoring. Fluorine-18 is produced from the liquid target reaction:

$$O^{18} \rightarrow (p,n) \rightarrow F^{18} \qquad (1)$$

This nomenclature is used to denote oxygen-18 as the target material and fluorine-18 as the product as a result of neutron capture when under a beam of energetic protons.
The solid target copper-64 reaction is :

$$Ni^{64} \rightarrow (p,n) \rightarrow Cu^{64} \qquad (2)$$

3.2.2. Reaction Rate

The production rate of a nuclear reaction will determine the practicality of using that reaction to produce the isotope. If the production rate is low, the cyclotron would need to run longer to produce the required quantity, thus impacting the production run of the following isotope.

The nuclear reaction production rate is a function of the proton energy, current density and target material [7]. The production rate of any reaction is a function of the cross section of the reaction. To characterize the probability that a certain nuclear reaction will take place, it is customary to define an effective size of the nucleus for that reaction, called a cross section, which is defined by :

$$\sigma = \frac{R}{I} \tag{3}$$

Where :

$\sigma =$ cross section

$I =$ number of incident particles per unit time per unit area

$R =$ number of reactions per unit time per nucleus

It must be noted that, the cross section is on the order of the square of the nuclear radius. A commonly used unit is the barn

1 barn = $10^{-28} m^2$

For copper-64 the nuclear reaction cross section at energies up to 14 MeV is shown in Figure 1 [8] with the units of cross section as millibarns. The data in Figure 1 is experimentally determined based on the research as indicated on the graph.

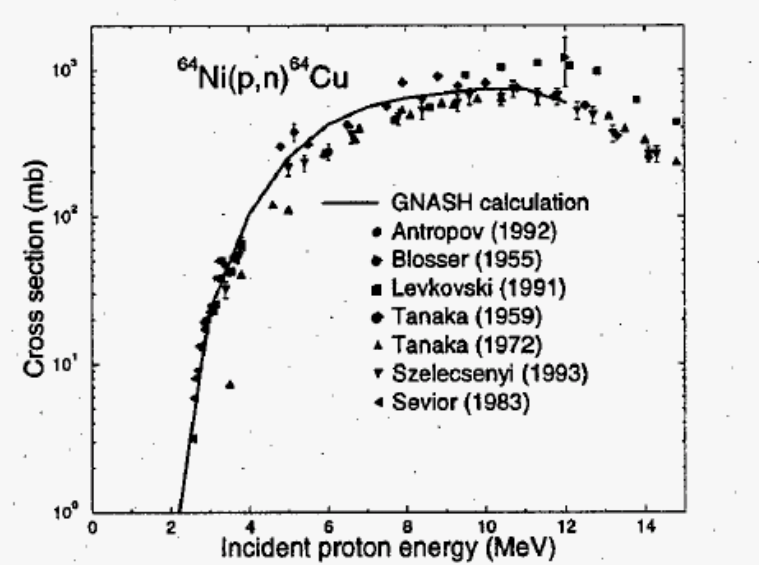

Figure 1 : Cross Section for Ni64(p,n)Cu64

As can be seen in Figure 1, the production rate for the nickel-64 (p,n) copper-64 reaction is maximum in the energy range from 9 to 12 MeV [8]. The theoretical production rate for this reaction is determined by integrating the cross section curve.

3.2.3. Energy Input

For all target types, the key performance parameter is the ability to effectively remove the heat deposited during the proton bombardment. The heat input can be calculated from the beam current and proton energy as shown below:

$$1\mu A = 10^{-6}\frac{C}{s} = \frac{10^{-6}\frac{C}{s}}{1.6x10^{-19}\frac{C}{p^+}} = 6.25\text{x}10^{12}\ \frac{p^+}{s} \qquad (4)$$

$$\dot{Q}(watts) = E(\frac{MeV}{p^+}) \text{ x } I(\mu A) \text{ x } \frac{6.25x10^{12}\ \frac{p^+}{s}}{1\mu A} \text{ x } \frac{1.6x10^{-13}J}{MeV} = 1(\frac{J}{s}) \qquad (5)$$

$$\dot{Q}(watts) = E(MeV) \text{ x } I(\mu A) \qquad (6)$$

This relationship indicates that the power input (watts) from a proton bombardment is the product of the proton energy (MeV) and the proton current (uA). The proton current is the number of protons per second that interact with the target material. An 11MeV beam of protons at 60 uA produces 660 watts of energy conversion. As can be seen, increasing the proton current increases the heat load, but also is necessary to increase the production of the desired isotope.

3.2.4. Solid Target Processing

The typical process for the production of a solid target involves plating a thin layer (around 0.1 mm) of target material onto a target support [9]. The target material is typically an enriched naturally occurring material. The enrichment process typically increases the production cost of the target material. The target disk provides the support for the target material as well as the interface to the seals and cooling system needed for operation. The target disk is then bombarded with energetic protons and the nuclear reaction occurs. The reaction converts only a small percentage of the enriched target material into the product isotope, with the remaining target material being available for reclaim. The radioactive target disk is typically placed in an acid solution to remove the plating [5]. The solution is then processed and neutralized and the product is attached to a biological molecule of interest. The unused enriched target material is reclaimed and used to plate the next target disk.

3.2.5. Proton Interaction

In nuclear physics, charged particles moving through matter interact with the electrons of atoms in the material. The interaction excites or ionizes the atoms, which leads to an energy loss as given by the Bethe formula [12]. The Bethe formula describes the energy loss per distance traveled of charged particles passing through matter [13]. This is also the resultant stopping power of the material.

The proton enters the target with an initial kinetic energy. After undergoing Coulombic interactions and radiation losses (bremsstrahlung), the kinetic energy of the proton is reduced after traveling a distance x along its path. Stopping power is defined as incremental energy lost (dE) per unit distance traveled (dx), or (-dE/dx). As the proton decelerates the stopping power increases further back into the target, reaches a peak, and drops off to zero [12].

The relativistic version of the Bethe formula is given by:

$$-\frac{dE}{dx} = \frac{4\pi}{m_e c^2} \cdot \frac{nz^2}{\beta^2} \cdot \left(\frac{e^2}{4\pi\varepsilon_0}\right)^2 \cdot \left[\ln\left(\frac{2m_e c^2 \beta^2}{I \cdot (1-\beta^2)}\right) - \beta^2\right] \qquad (7)$$

Where :

$$\beta = \frac{v}{c}$$

$\upsilon =$ velocity of the particle

$E =$ energy of the particle

$x =$ = distance traveled by the particle

$c =$ speed of light

$z =$ particle charge

$e =$ charge of the electron

$m_e =$ rest mass of the electron

$n =$ electron density of the target

$I =$ mean excitation potential of the target

$\varepsilon_0 =$ vacuum permittivity

For low energies where the velocity of the particle is small ($\beta << 1$), the Bethe equation simplifies to :

$$-\frac{dE}{dx} = \frac{4\pi n z^2}{m_e v^2} \cdot \left(\frac{e^2}{4\pi\varepsilon_0}\right)^2 \cdot \left[\ln\left(\frac{2m_e v^2}{I}\right)\right] \qquad (8)$$

Here the electron density can be calculated by:

$$n = \frac{NaZ\rho}{AM_u} \qquad (9)$$

Where :

$Na =$ Avagadro's number

Z = atomic number

$\rho =$ Density

$A =$ mass number

$M_u =$ mass molar constant

The National Institute of Standards and Technology maintains a database (PSTAR) which can be used to calculate the penetration range in various materials for protons. For proton energies above 0.5 MeV, the database utilizes the Bethe formula to generate the penetration ranges. The range of protons interacting with elemental gold and nickel are shown in Figures 2 and 3 respectively.

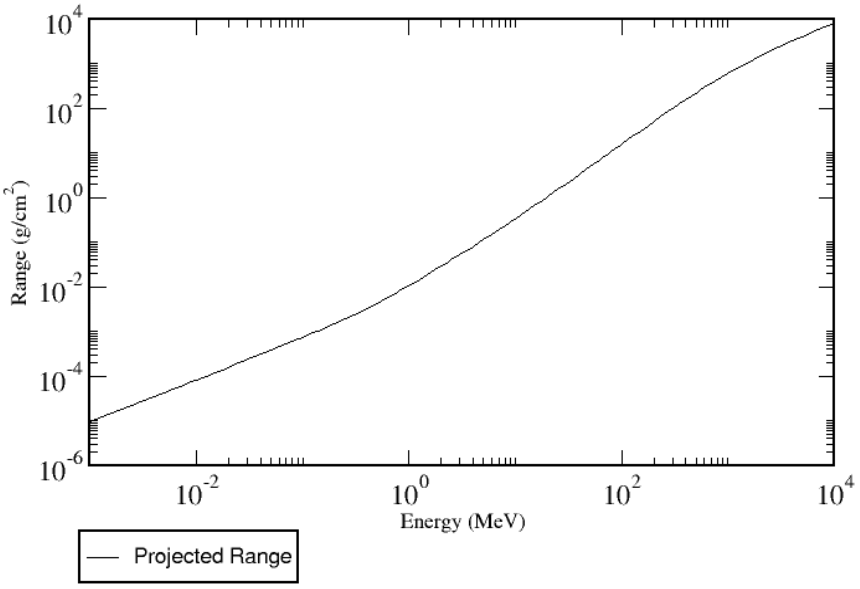

Figure 2 : Range of Protons in Gold

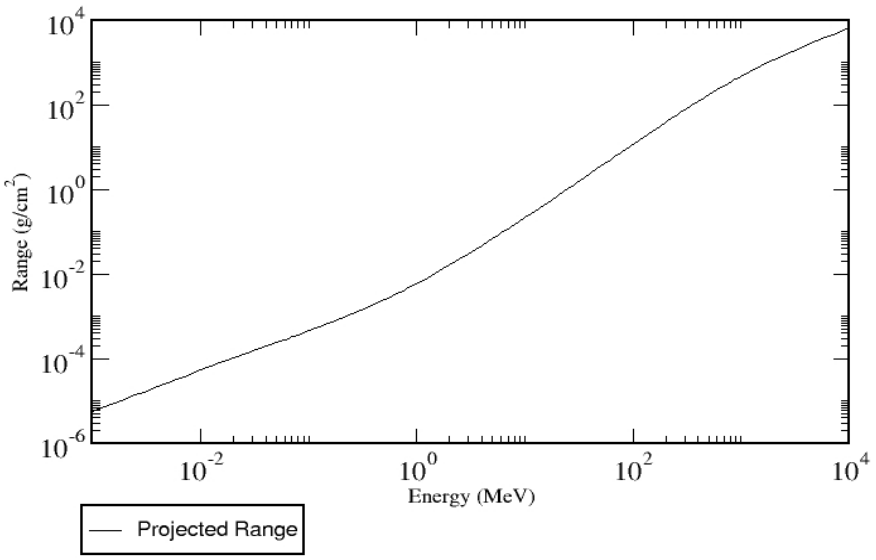

Figure 3 : Range of Protons in Nickel

The y-axis data is the penetration range in the units of g/cm^2 and the x-axis is a range of proton energy. In order to determine the distance in cm, it is necessary to divide the penetration range by the density of the material. The data is collected in Table 2.

Table 2 : Proton Penetration

Material	Range (g/cm^2)	Density (g/cm^3)	Penetration Distance (cm)
Gold	0.3922	19.3	0.0203
Nickel	0.2551	8.9	0.0287

As can be seen from the data in Table 2, protons with an initial energy of 11MeV will penetrate 0.203 mm in gold and 0.287 mm in nickel. Since the enriched plated nickel is typically 0.1 mm thick, the proton beam passes through the nickel and deposits the majority of its energy upon stopping in the gold support disk.

The protons deposit energy in a non-linear fashion as they penetrate into the target disk material. The data from the NIST PSTAR program can be used to calculate the change in energy per change in distance (dE/dx) and then graphed relative to the penetration distance. The resulting graph is the Bragg curve, with the dramatic rise in dE/dx at the end of the penetration distance identified as the Bragg peak. This graph, shown in Figure 4 illustrates that the majority of the heat load is deposited near the maximum penetration distance.

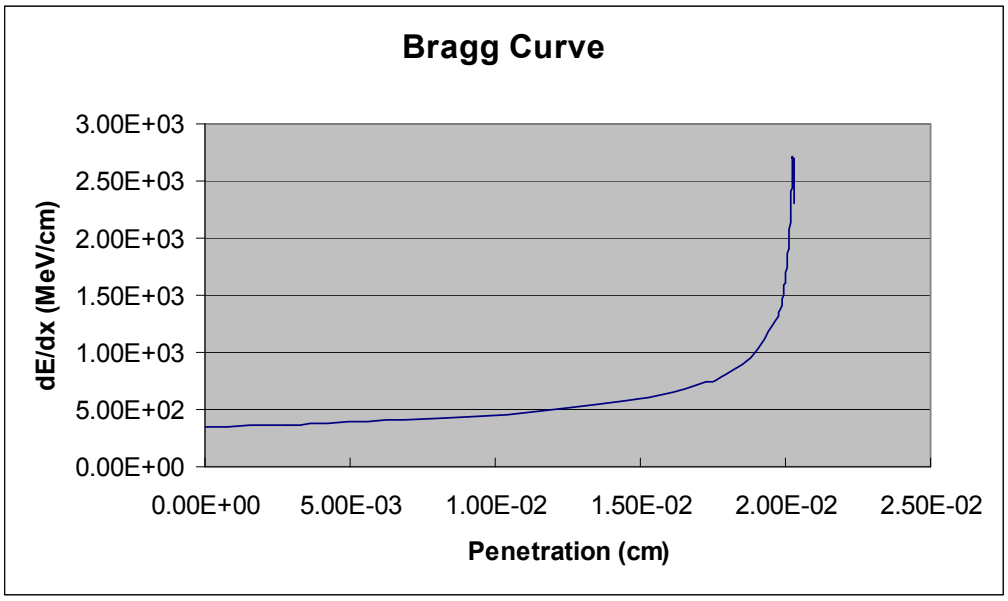

Figure 4: Bragg Curve

3.3. Materials

3.3.1. Target and Support

The target material for the production of copper-64 is naturally occurring nickel 64 isotope [4]. Nickel 64 enriched to greater than 90 % purity is expensive and thus targets are typically fabricated with a thin layer of nickel plated onto a more substantial target

disk. Physical and chemical properties must be taken in to account when choosing a material for the target disk. For example, some applications require the material of the plate to be resistant to acidic solutions, especially when wet chemistry is necessary for the separation of the radioactive product from the target material. In cases where a dry distillation process is required for the separation of the product, materials that do not react with the target material at high temperatures are preferred. Another important issue to be considered when choosing a target disk is the proton activation of the material. Note that all materials will suffer activation at different levels with different half-lives and associated radiation fields of the activated products. However, this problem can be mitigated by careful selection of the target support As a result, target disks are typically fabricated from non reactive noble metals such as gold or platinum.

3.3.2. Machined Parts

The machined parts which hold or transport the target disk in the target changer must be as non reactive as possible to the gamma and neutron fields created during the bombardment. They must also have good cooling properties and be non reactive to de-ionized water, which is used for target cooling. They should have excellent machining properties, be capable of attaining a good surface finish, and have sufficient mechanical properties for the structural requirements. A typical material for these components is 6061 aluminum alloy.

3.3.3. Seals

The sealing materials must stand up to the gamma and neutron fields as well. They must have low out gassing properties due to their exposure to the high vacuum areas. They must have thermal properties that prevent them from deforming or melting during bombardment, and they should be inert to all chemicals they may contact during normal

operation. The BL grade of the fluoroelastomer Viton has the appropriate properties for most uses in target design.

3.4. Thermal

3.4.1. Introduction

Heat is deposited at and below the surface of the target by the energetic proton bombardment. The heat deposition is linear with beam current, thus the amount of heat that can be effectively handled by the target design directly affects the production capacity of the target. A common method of dealing with poor thermal design is to limit the beam current to very low levels [10]. Thus, in order to meet the required production rates, it is necessary to optimize this design to withstand the maximum beam current that can be produced on the cyclotron. The high vapor pressure of the thinly plated target material mandates a maximum temperature well below the melting point of the target material or the target disk [10]. For the materials used in this work, the melting point of gold is 1059 ^{o}C and nickel is 1453 ^{o}C. The configuration of the target disk relative to the proton beam and cooling is shown in Figure 5.

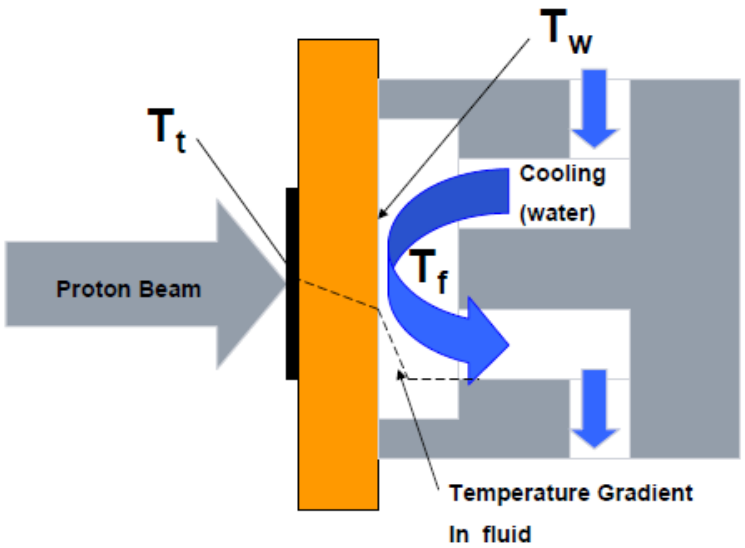

Figure 5 : Target Cooling

Where :

T_t = temperature of the target disk wall on the target side

T_f = temperature of the cooling fluid, typically 7 ^{o}C

T_w = temperature of the target disk wall on the cooling side

As can be seen from Figure 4, the proton beam impacts the front of the target, passing through the nickel-64 and depositing energy in the target disk. The front side of the target disk is in high vacuum with typical values for the vacuum level of 5 x 10^{-6} torr. The cooling processes are conduction through the target disk, and forced convection from the target disk to the circulating cooling fluid. The cooling fluid is maintained at 7 ^{o}C by an external dual pass heat exchanger.

A one dimensional thermal analysis will be performed to determine if designing to the operational current limit of 60 μA is feasible with the given cooling fluid, temperature and flow rate. This will guide the development of the design by indicating if the desired approach of interfacing to the existing install base of cyclotrons is a practical avenue to pursue.

3.4.2. Conduction

The thickness of the plate support will be kept as thin as practicable possible to facilitate the heat dissipation, but thick enough to guarantee sufficient mechanical strength to withstand the pressure of the cooling water and the structural rigidity to compress the sealing materials. Efficient cooling for this dynamic system requires that the plate support be made of a material with a high thermal conductivity and low heat capacity

[10]. Usually, materials with high conductivity to capacity ratio are desirable to efficiently remove the heat generated by the beam power on the target support.

Fourier's Law of Heat Conduction for an isotropic material can be stated as [11]:

$$Q = -K\nabla T \tag{10}$$

Where :

$Q =$ heat flux , $\frac{W}{m^2}$

$K =$ thermal conductivity of the material , $\frac{W}{mK}$

$\nabla T =$ temperature gradient in 3 dimensions , $\frac{K}{m}$

In order to determine the feasibility of cooling the target in the defined conditions available, a one dimensional approximation in the x direction was performed. The x direction is defined as along the axis of the incoming proton beam. In Cartesian coordinates, the x component of this equation is:

$$Q_x = -K\frac{\partial T}{\partial x} \tag{11}$$

If Since the heat flow is one-dimensional:

$$Q_x A_x = -KA_x \frac{dT}{dx} \tag{12}$$

Since the heat transmission is steady and the thermal conductivity of the material and thickness are constant, the above equation becomes:

$$q = \frac{KA\Delta T}{L} \tag{13}$$

Where:

$q =$ heat input , *w*

$K =$ thermal conductivity of target disk material , $\frac{w}{m - C}$

$\Delta T = Tt - Tw,\ C$

$L =$ thickness of the target disk, m

$A =$ area of heat input normal to the x direction, m^2

Table 3 shows the calculated temperature differential across the target disk based on varying beam currents and target disk material. The target disk materials included in the table are the most commonly utilized noble metals for this application due to their high thermal conductivity and their non-reactive properties when exposed to the chemicals used in the plating and dissolution processes. The beam area is based on the collimated beam size of 10 mm diameter.

Table 3 : Conduction Calculations

Energy (MeV)	Current (uA)	Q (w)	Material	K (w/m-C)	Thickness (m)	Beam Area (m2)	Temperature differential (C)
11	20	220	Gold	318	0.002	0.0000785	17.6
11	40	440	Gold	318	0.002	0.0000785	35.3
11	60	660	Gold	318	0.002	0.0000785	52.9
11	20	220	Silver	429	0.002	0.0000785	13.1
11	40	440	Silver	429	0.002	0.0000785	26.1
11	60	660	Silver	429	0.002	0.0000785	39.2
11	20	220	Platinum	73	0.002	0.0000785	76.8
11	40	440	Platinum	73	0.002	0.0000785	153.6
11	60	660	Platinum	73	0.002	0.0000785	230.3

The temperature differential is the calculated value across the target disk. The optimal current is 60 uA, as this is currently the maximum output from the cyclotron. From the data in this table, the most applicable target disk material could be either gold or silver. From a chemical reactivity viewpoint, gold is less than half as reactive as silver, so it is the preferred option. Thus the data in Table 2 indicate that at a full beam current of 60 μ A, there will be a 52.9 ^{o}C temperature differential from the target side of the disk to the cooling side of the disk.

3.4.3. Convection

The target disk is cooled by water impinging at 90^{o} on the back or non-target side. The water is de-ionized and cooled to 7 ^{o}C , with an available flow rate of 0.5 gallons/minute. The cooling water is directed onto the back of the target disk so that it acts as a submerged jet arrangement. For all studies performed it has been shown that, for a constant jet diameter, heat transfer increases with increasing Reynolds number (Re) , with the Nusselt number (Nu) proportional to Re $^{0.5 \text{ to } 0.8}$.

Convection is described by Newton's law of cooling, which states that the rate of heat loss of a body is proportional to the difference in temperatures between the body and its surroundings.

$$q = hA\Delta T \qquad (14)$$

Where :

$q =$ heat input , *w*

$h =$ coefficient of convective heat transfer , $\frac{W}{m^2 -^o C}$

$A =$ surface area of heat transfer, m^2

$\Delta T = (T_w - T_f)$, ºC

The convective heat transfer coefficient depends upon physical properties of the fluid such as temperature and the physical situation in which convection occurs. Therefore, the heat transfer coefficient must be derived or found experimentally for every system analyzed. Formulas and correlations are available in many references to calculate heat transfer coefficients for typical configurations and fluids. For laminar flows, the heat transfer coefficient is rather low compared to the turbulent flows; this is due to turbulent flows having a thinner stagnant fluid film layer on heat transfer surface. For this application, the value for h will be estimated from the definition of the Nusselt number:

$$h = \frac{Nu}{L} K_{water} \qquad (15)$$

Where :

$Nu =$ Nusselt's number

$K_{water} =$ thermal conductivity of water = 0.58 $\frac{W}{m -^o C}$

$L =$ length of flow , m

The Nusselt number is the ratio of convective to conductive heat transfer across the boundary. A large Nusselt number, between 100 -1000, corresponds to more active convective heat transfer. For forced convection, the Nusselt number is a function of the Reynolds number and the Prandtl number. The Nusselt number for this application will be estimated from the Dittus-Boelter equation as shown in equation (16). The Dittus-Boelter equation is valid for 0.7 < Pr <160 and Re > ~10,000. This estimation of the heat transfer coefficient will be conservative in that it is for flow in a smooth pipe and the actual configuration of flow onto the target disk is a submerged jet arrangement more likely to disturb the thermal boundary layer.

$$Nu_D = 0.023\,\mathrm{Re}^{0.8}\,\mathrm{Pr}^{0.4} \tag{16}$$

Where :

$$\mathrm{Re} = VL\frac{\rho}{\mu} \tag{17}$$

$$\mathrm{Pr} = C_p\frac{\mu}{K} \tag{18}$$

Where :

$V =$ velocity of water flow , $\frac{m}{s}$

L =length of flow *, m, = .003 m for this application*

$K =$ thermal conductivity of water = 0.58 $\frac{w}{m-C}$

$\rho =$ density of water = 1000 $\frac{kg}{m^3}$

$\mu =$ viscosity of water = .001 $\frac{kg}{m-s}$ at 20 ^{o}C

$C_p =$ specific heat of water = 4186 $\frac{J}{kg-C}$

By calculation, Pr = 7.217. The velocity component of the Reynolds number is calculated by treating the port that routes cooling water onto the back of the target disk as an orifice flow.

$$V = \frac{Q}{Ak} \tag{19}$$

Where :

$A =$ area of orifice

$k =$ orifice geometry factor = 0.82

Table 4 provides the results of calculations with varying cooling flow rate and orifice size.

Table 4 : Convective Heat Transfer Coefficient Calculations

Volumetric flow rate (gpm)	Volumetric flow rate (m3/s)	Orifice size (mm)	V (m/s)	Re	Nu	h (w/m2C)
0.5	3.15E-05	3.0	5.44	19031	134	22284
0.5	3.15E-05	3.5	3.99	13982	105	17413
0.5	3.15E-05	4.0	3.06	10705	85	14063

The values for the coefficient of heat transfer from Table 4 , were then used to generate the temperature differentials in Table 5.

Table 5 : Summary Temperature Calculations

h (w/C)	Q (w)	A (m2)	Water (°C)	delta t (°C)	Tw(°C)	Tt (°C)
22284	660	0.0001266	7	233.9	240.9	293.8
17413	660	0.0001266	7	299.4	306.4	359.3
14063	660	0.0001266	7	370.7	377.7	430.6

From the results in Table 5 , it can be seen that the expected temperature on the target side of the target disk ranges from 293.8 ^{o}C to 430.6 ^{o}C depending on orifice size.

The one dimensional approximation provides the basic understanding of the impact of the orifice size and flow rate on the thermal design. With an orifice size of 3.5 mm diameter and gold as a material, the project temperature profile is:

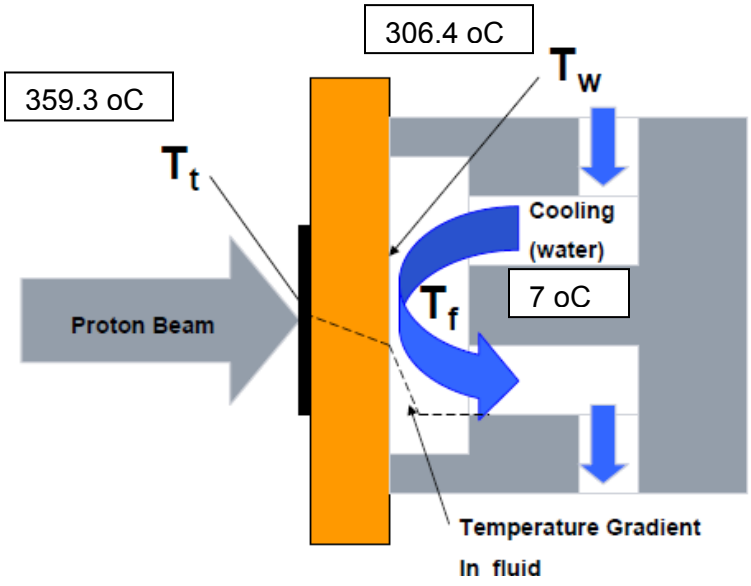

Figure 6 : Final Temperature Profile

The result of the thermal analysis indicates that operation of the target system at full current should produce a maximum temperature that has a ‘safety factor’ of approximately 3 times the melting temperature of gold.

3.5. Mechanical

3.5.1. Overview

The design of the solid target system needed to take into account several operating envelopes in order to be successful in accomplishing the design intent of enabling the wide spread production of solid target products. First, the system must fit within an existing operating space. The target system and any required support equipment must physically fit inside the moveable shielded enclosure around the cyclotron. It must also allow the simultaneous operation of standard liquid and gas targets. The design must allow as much remote or automatic handling process as possible in order to reduce radiation exposure to personnel. And finally, the design must function at a beam current that makes practical amounts of isotope, while being cooled by an existing cooling supply system.

3.5.2. Alternate Designs

In the process of researching the best design solution, several design approaches were considered. An initial concept was to attach the target disk into a carrier insert that would fit within an existing target carousel. The benefit of this design would be a small operating envelope and the repeatability of target sealing during bombardment.. This design had the serious limitation of not allowing the target disk to be remotely removed once proton bombardment was complete. This would potentially expose operators to

excessive radiation as they worked to disassemble the irradiated target disk. Also, an extra set of seals would have been required to perform the sealing operations. The target disk would have been sealed within its holder, and then the holder would have been sealed to interface to the existing target carousel.

A second design concept was to have an external mechanism which could be loaded and unloaded remotely, while translating the target disk into the target carousel. While this concept solved most of the design limitations, it had several negative features. The mechanism would not fit within the moveable shielded enclosure, and would have required a special shield insert. This would have limited the ability to retrofit the design onto existing cyclotrons due to the cost of shield installation and the down time required. In addition, this concept could not interface to the existing vacuum system. Modifying the vacuum system would have limited the target carousel to solid target only operation.

3.5.3. Design Description

The successful design was initiated with modification to the basic target carousel. If the required mechanisms could be incorporated into this envelope, it would enable the automatic position control system to function the same as currently designed. It would also provide the interface to the existing cooling system, compressed air system and vacuum system. The mechanism utilized would fit within a portion of the target carousel without disturbing the cooling paths or utility arrangements needed to support the current liquid of gas targets. The new mechanism would not extend beyond the envelope of the existing target carousel and thus have no interference with the moveable shielding.

The design that accomplished all of the key design requirements is illustrated in Figure 7 with key components of the design identified in the figure.

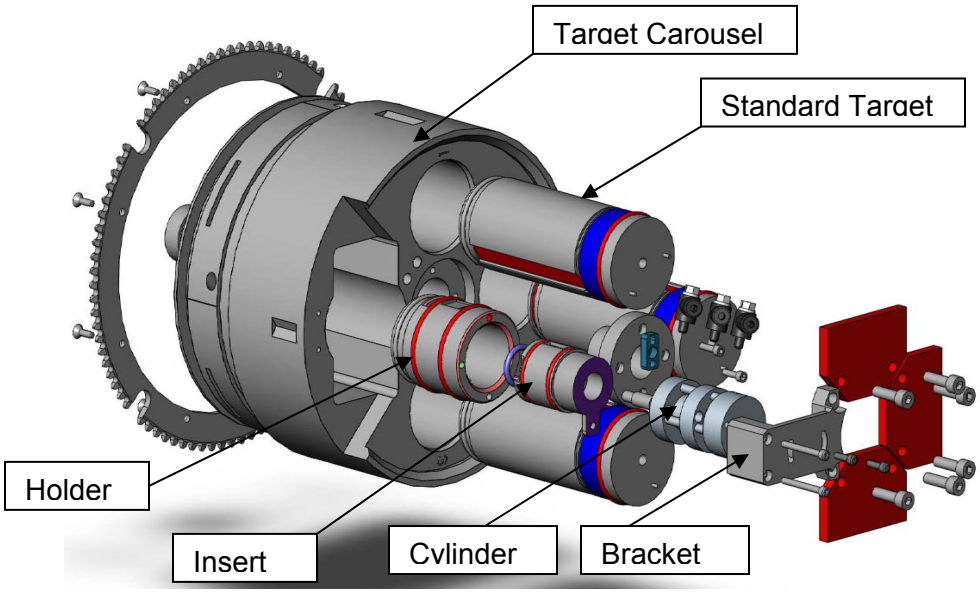

Figure 7 : Solid Target Assembly

The target carousel was modified to accept the solid target mechanism. The placement of the target disk is a manual operation because prior to bombardment there is no risk from radiation exposure. In order to introduce the target disk into the target port , a slot was machined into the modified target carousel that was slightly larger than the target disk. This slot is shown in Figures 8 and 9. The slot allows the target disk to be dropped into and fall out of the target carousel, while not crossing any of the internal water cooling or vacuum paths. Due to the critical dimensions of the slot and its depth , the proposed machining method is electro discharge machining (EDM).

The target carousel also provides the alignment detents for software controlled positioning of the target changer. The alignment detents interface to an array of three detent switches. The pattern of these switches is coded to represent a target position in

the software control system. These detent locations are used when the target changer carousel is rotated in operation from the service port position to the beam port position. The service port allows the target in that position to be removed and serviced without affecting the main cyclotron vacuum level. The target changer carousel incorporates a series of face seal o-rings that establish three different and isolated vacuum zones. The alignment detents are identified in Figure 8.

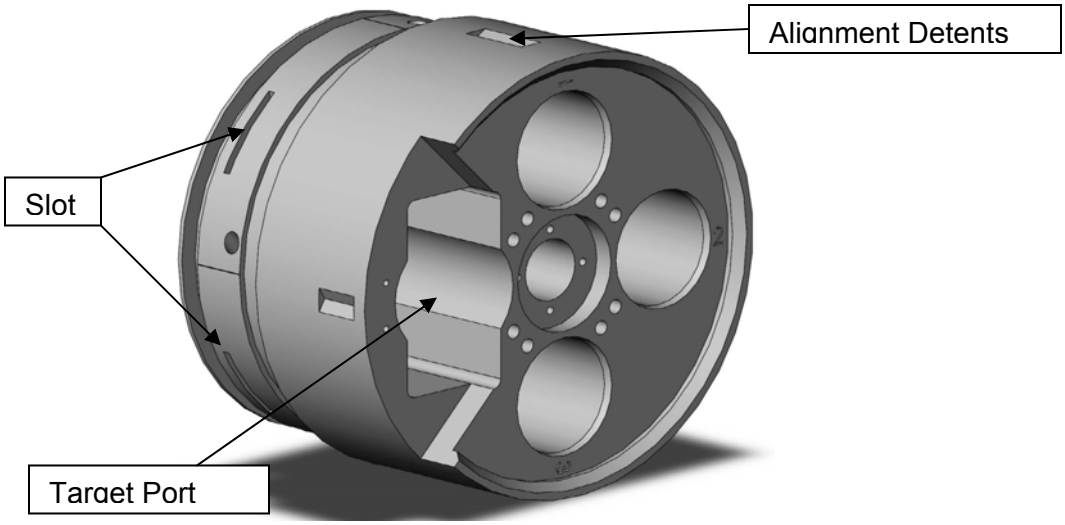

Figure 8 : Modified Target Carousel

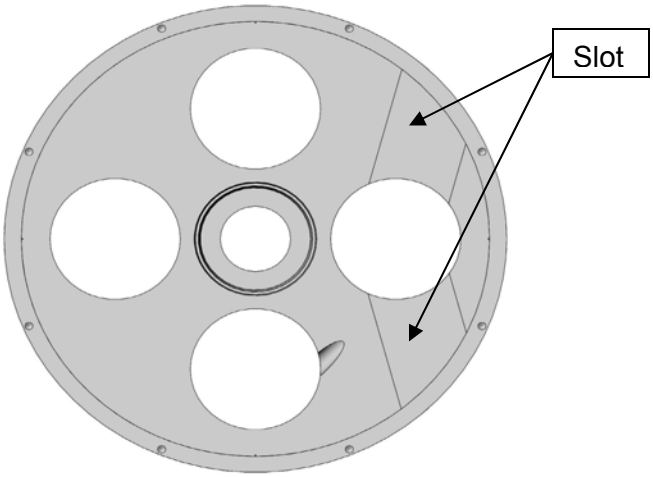

Figure 9 : Access Slots

The holder is an aluminum piece which has been machined from a solid billet. The function of the holder is to provide the cooling channels to route the cooling water onto the target disk, align the insert, and provide a matching slot to the target carousel. The internal diameter of the holder is key to proper operation of the system. The bore alignment and surface finish were tightly controlled. The entrance to the slot is chamfered to allow some misalignment between the insert and target carousel. The key features of the insert are identified in Figure 10.

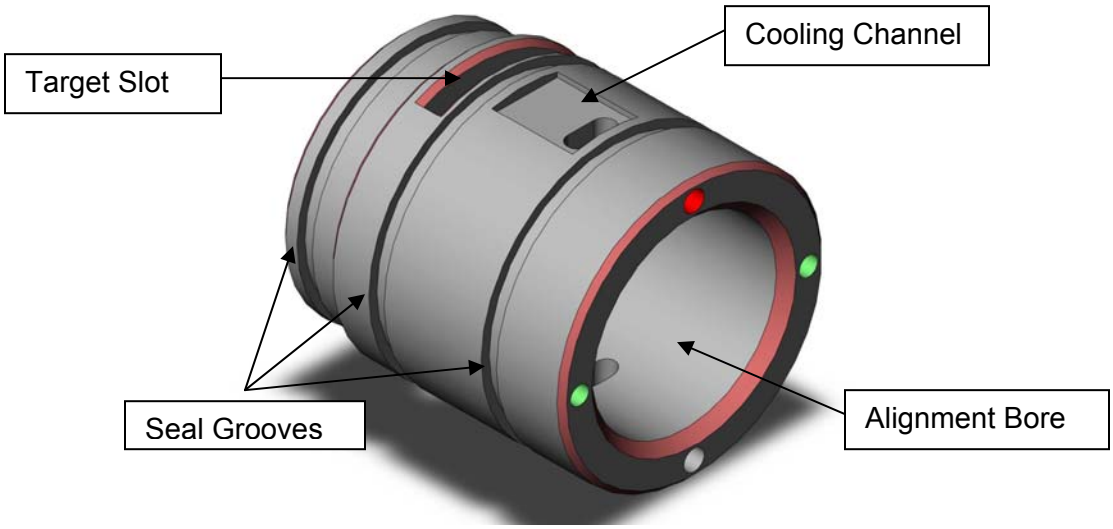

Figure 10 : Holder

The insert performs several functions in the design of the solid target system. The insert provides a protrusion that locates the target disk as it is loaded through the slot. When the insert is located in the LOAD position, the protrusion blocks the slot from below and allows the target disk to slide into position.

The insert is attached to a three position cylinder, which allows the target disk to fall from the carousel when retracted. It also routes cooling water onto the target disk and provides the face seals. The air pressure which actuates the cylinder must be regulated so that the required axial force is available to compress the two seals. For the cross section and hardness of the seals, the compression force necessary for sealing is approximately 5 pounds per linear inch. This equates to a required force of 22 lbf. As the pneumatic cylinder piston area is 0.40 $inch^{2.}$, the supply pressure must be maintained above 55 psi for the system to seal properly. The cooling water channel is configured so that as the insert moves within the housing, cooling water continues to flow to the target disk. These features are identified in Figure 11:

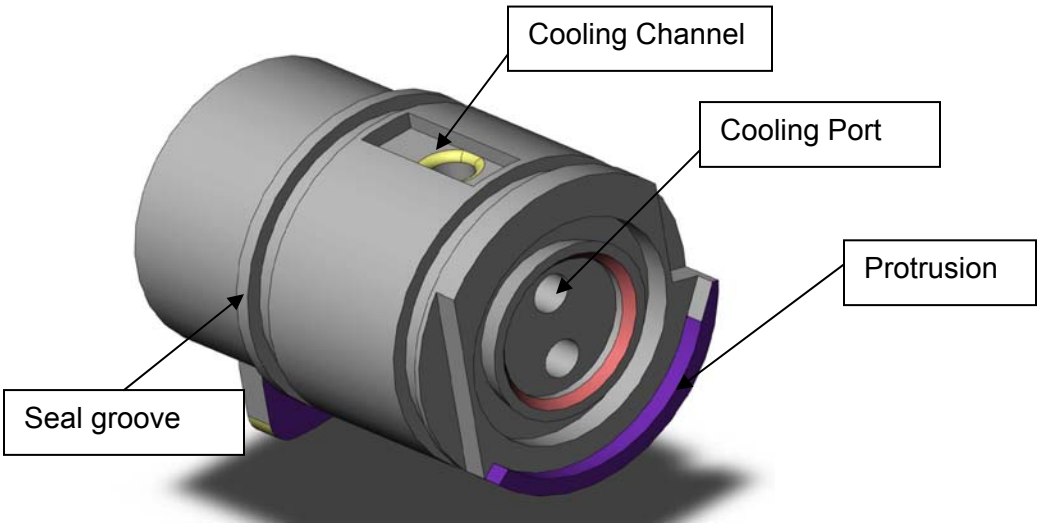

Figure 11 : Insert

The assembly and interfaces between the holder and the insert are shown in Figure 12. The path of the cooling water is indicated by the blue arrows. As the insert moves within the holder, from LOAD to COMPRESS to UNLOAD positions, the cooling water supply is maintained.

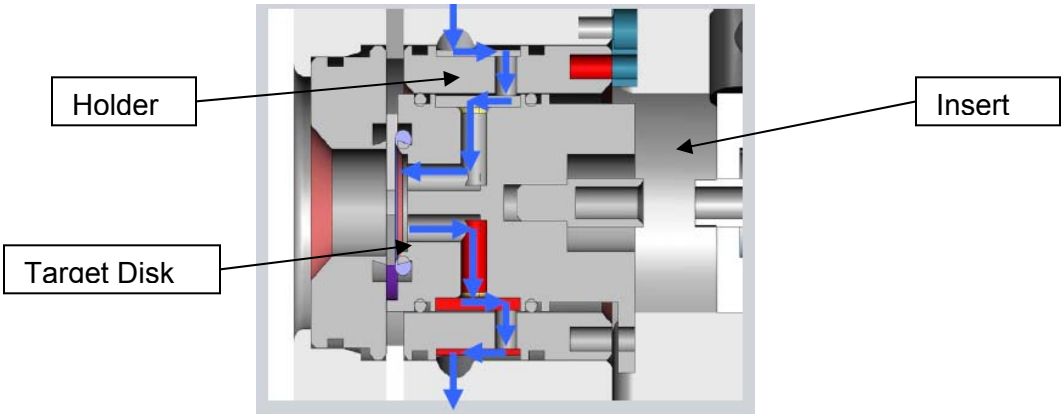

Figure 12 : Cooling Path

4. Operation

The operation of the solid target system is controlled from the existing cyclotron control software. Both automatic and manual operational modes are available. The graphical user interface (GUI) shows the status of valve positions, vacuum levels, and readiness for beam. Figure 13 shows a screen capture of the control system.

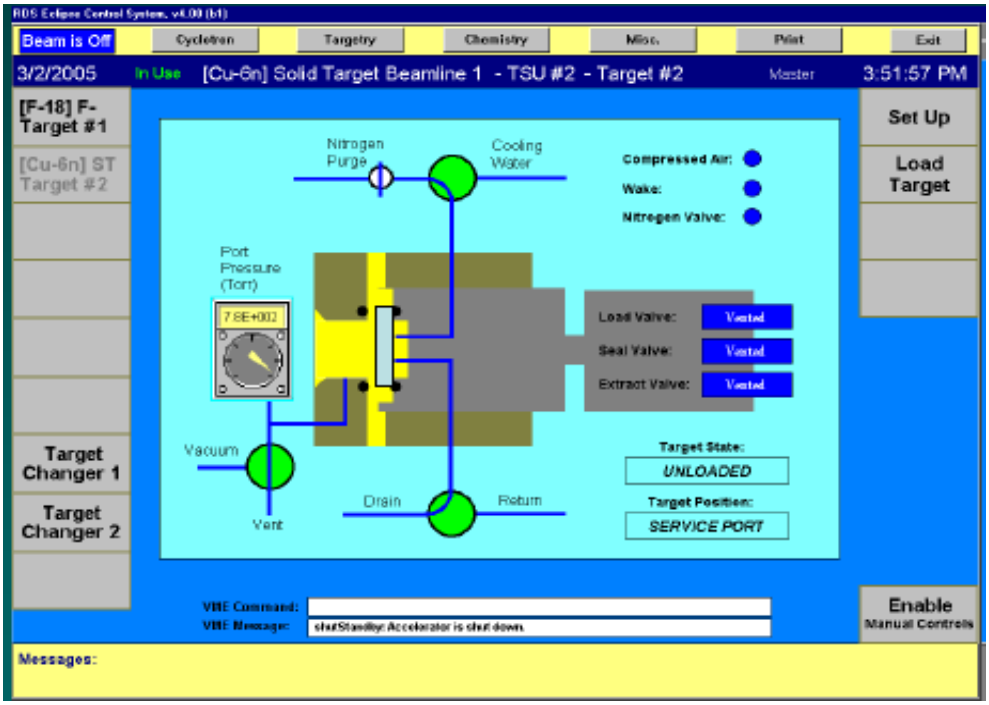

Figure 13 : Control System

The operation starts with preparing the cyclotron to receive the plated target disk. In order to open the shielded enclosure, the control system verifies that the proton beam is off. This is accomplished by removing power to the ion source bias supply so that no negative ions can be drawn into the accelerating region. Once this is verified, the operator can open the movable shielding and gain access to the target carousel.

In order to place the plated target disk into the carousel, the solid target position must be rotated to its service position as identified in Figure 14. The cooling water must then be rerouted to by pass the target carousel and the remaining water removed by pressurized air. These steps are controlled by the central control system actuating valves. Once the target carousel is dry, the service port vacuum can be relieved and brought to ambient pressure. The target carousel is now ready to receive the plated target disk.

The control system is used to place the insert into the LOAD position, where the protrusion blocks the slot and the insert is actuated by a three position pneumatic cylinder. The plated target disk is then loaded manually into the target carousel. As the target disk falls into the target carousel, this protrusion stops the disk and holds it in proper position.

The pneumatic cylinder is then actuated to compress the target disk between two o-ring seals. The seals are located on the face of the target carousel and in the insert. Once compressed, the target disk is sealed from vacuum on the beam side and from the cooling water on the back side. The seals are retained in their grooves by use of a single dovetail groove design. The vacuum and cooling water are now engaged by the control system.

The target is now ready to be moved into the beam port position. This is accomplished by rotating the target carousel in the target hub. A series of o-rings mange the vacuum levels as the target carousel rotates into position to prevent rapid loss of main tank vacuum.

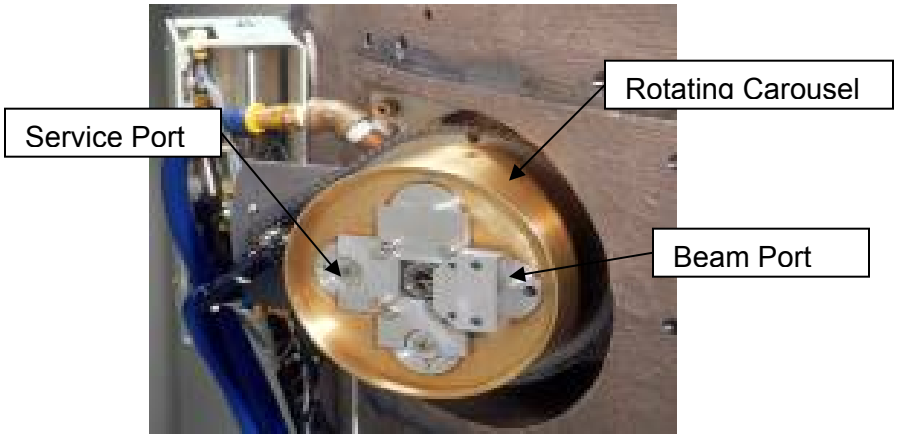

Figure 14 : Basic Carousel Arrangement

The target is now in the beam position and can be bombarded with protons. Bombardments of solid targets can vary from 1 hour to 12 hours depending on the nuclear reaction and production rate. After bombardment, the target disk is rotated back to the service port and the cooling water is stopped. The excess water removed by blowing compressed air through the system. The vacuum to the service port is then removed. The pneumatic cylinder is actuated to retract the insert so that the target disk is allowed to drop from the target carousel into a shielded container.

5. Testing and Results

5.1. Assembly and Bench Testing

In order to evaluate and validate the design, a testing plan was created which established criteria for applicable operational parameters and acceptable performance.

Detailed engineering prints were created for each of the components of the design as well as the overall assembly. The individual components of the assembly were fabricated and inspected to these prints. Upon receipt of the parts, they were cleaned per standard procedure for high vacuum use. This process involves ultrasonic immersion in a series of progressively weaker de-greasing agents.

The parts were assembled up to the level as shown in Figure 15. During assembly the fit of each part and its design parameters were carefully checked.

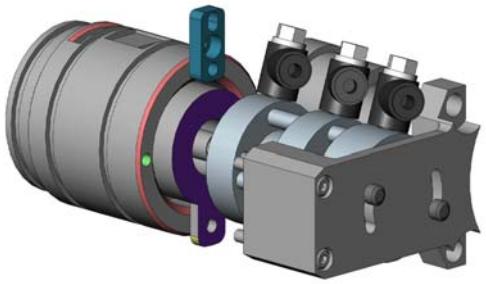

Figure 15 : Initial Assembly

This sub-assembly was then mounted into the modified target carousel, which was mounted onto a target changer test fixture. At this point, the target assembly was checked to ensure proper fit to the mounting assembly. Proper rotation and alignment was also verified. The service port was then connected to a vacuum pump and the vacuum integrity of the system was verified. During this portion of the testing, actuation

of the three position cylinder was performed by air pressure routed by the manipulation of a series of manual valves.

The completed assembly , which is shown in Figure 16, was removed from the test fixture and mounted on a beam port of an 11MeV proton cyclotron.

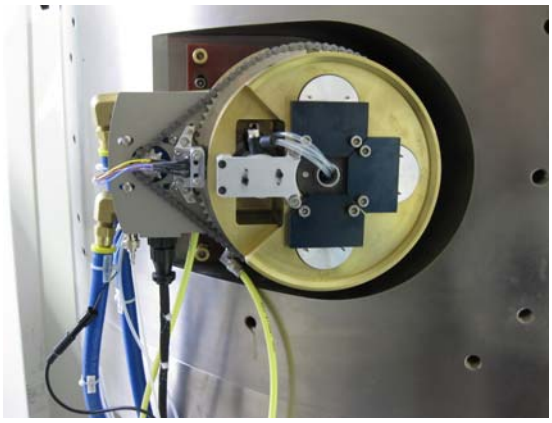

Figure 16 : Mounted Solid Target System

5.2. Cyclotron Testing

Cyclotron testing consisted of several phases. First the mechanical fit and operational verification was performed. This was accomplished by mounting the target assembly onto the cyclotron, while checking for alignment, fit and clearance issues. At this point , the water cooling supply and return hoses were connected and checked for clearance. The electrical connections were made and communication with the central cyclotron control system was verified. The shields were moved from open to closed position while checking for interferences or clearance issues.

The functional testing of the solid target system consisted of controlling the system from the control computer and loading the target disk, compressing the target disk, unloading the target disk. The action sequence was performed 25 times without failure.

The next phase of testing was the high vacuum integrity testing. The cyclotron main tank vacuum was opened into the target changer and vacuum levels were recorded . The cooling water was turned on to the target changer. It is important to check the vacuum levels with the cooling water flowing to both verify the water seals and the performance of the seals at operational temperature. The target position was rotated from the service port into the beam port. The target changer position was then rotated from the beam port back to the service port. The cooling water was rerouted to bypass the target changer carousel and the residual water was removed by compressed air. The various valves required to perform these operations were controlled by automatic code from the central control computer. The service port vacuum was then vented and the target automatically unloaded. The results are recorded in Table 6 .

Table 6 : Vacuum Testing Results

Test	Service port Vacuum level (torr)	Main tank vacuum level (torr)	Target extraction successful
1	0.18	2.0 x 10-7	Yes
2	0.23	1.8 x 10-7	Yes
3	0.24	1.6 x 10-7	Yes
4	0.25	1.6 x 10-7	Yes
5	0.25	1.6 x 10-7	Yes
6	0.24	1.6 x 10-7	Yes
7	0.26	1.6 x 10-7	Yes
8	0.27	1.5 x 10-7	Yes
9	0.24	1.5 x 10-7	Yes
10	0.25	1.5 x 10-7	Yes

The final phase of cyclotron testing was bombardment of the target disk with energetic protons. The evaluation criteria were the integrity of the main tank vacuum, lack of damage to the seals and target disk surface. The main tank vacuum was monitored and recorded before and during the testing. The target surface and seals were examined and after each run was complete. The results are listed in Table 7.

Table 7 : Beam Testing Results

Test	Current (uA)	Time (min)	Vacuum Integrity	Seal damage	Target surface finish
1	20	15	OK	None	OK
2	20	30	OK	None	OK
3	20	60	OK	None	OK
4	40	30	OK	None	OK
5	40	60	OK	None	OK
6	40	90	OK	None	OK
7	60	30	OK	None	OK
8	60	60	OK	None	OK
9	60	90	OK	None	OK
10	60	120	OK	None	OK

At one point in the cyclotron testing, the cooling water flow into the target changer was restricted from the expected 0.5 gpm to 0.25 gpm. This operational run at 60 uA for 1 hour resulted in a slight deformation of the target disk on the beam side. The surface of the target disk showed indication that the temperature had become close to the melt temperature of the material. When the flow of 0.25 gpm was used to calculate the expected temperature of the beam side, the one dimensional model produced a resultant temperature of 581 ^{o}C. This unplanned experiment indicated the safety margin of the model is closer to 2 times the melt temperature of the material. The variation in

safety factor is most likely due to the 0.20 mm deep location of the majority of the heat load.

5.3. Operational Testing

After completing bench and cyclotron testing, the prototype solid target assembly was cleaned, packed and shipped for installation at the Fukui University Medical Center in Fukui Japan. Fukui University supplied the processing expertise and equipment to complete the operational testing of the target assembly by producing the plated target disks as well as the post bombardment chemical processing for the copper-64 isotope.

The solid target assembly was installed on beamline #1 of the existing 11 MeV cyclotron. The cyclotron based tests as described in section 5.2 were repeated, with no issues identified. The installation is shown in Figure 17.

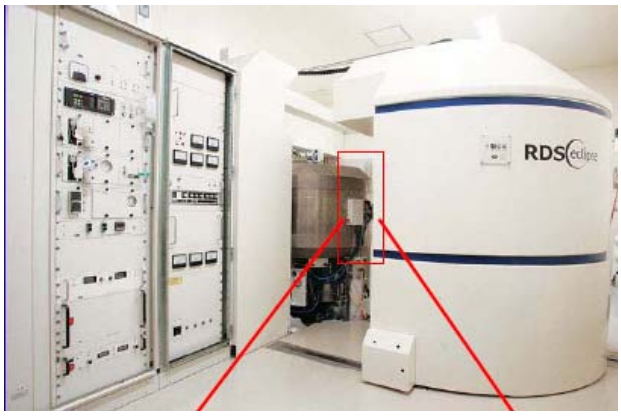

Figure 17 : Cyclotron Installation

Target disks plated with approximately 100 μm thickness of nickel-64 were prepared by the process optimized at Fukui University. A typical target disk is shown in Figure 18.

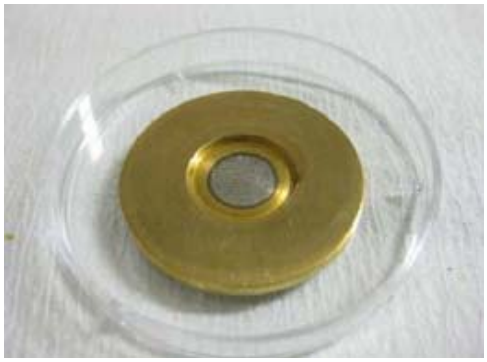

Figure 18 : Plated Target Disk

A plated target disk was loaded into the solid target system and rotated into the beam port position. The target disk was bombarded with protons at a beam current of 40 μA for 1 hour. The target disk was then rotated to the service port position and automatically released from the target carousel, where it was allowed to drop into a shielded carrying container placed inside the moveable shielded enclosure. The target disk was manually transported to a shielded processing enclosure where the dissolution and chemistry process for the copper-64 isotope was performed. This experiment was repeated 11 times with the production data summarized in Figure 19. The data is for copper-64 production rates in mCi/uA-hr at End of Beam (EOB) based on thickness of the plated target material in μm. As can be seen, there is a general relationship between increasing target thickness and increasing isotope production. This is expected since increasing target thickness provides more material for nuclear reactions to occur. Since all experiments were performed at 40 μA for 1 hour, the amount of copper-64 produced was typically 30 mCi at EOB as shown where A = final activity:

$$A = 0.75\frac{mCi}{\mu A \cdot hr} \cdot 40\mu A \cdot 1hr = 30mCi$$

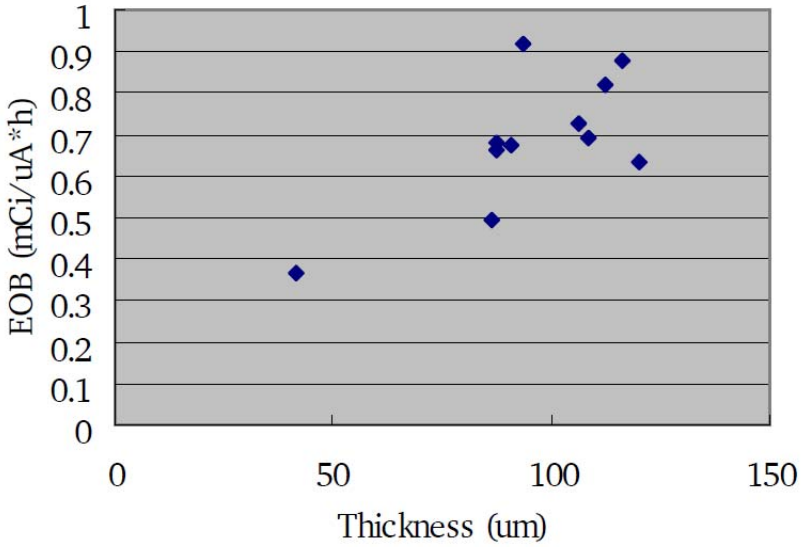

Figure 19 : Results from Copper-64 Testing

6. Summary and Conclusions

The purpose of this work is to design a mechanism that would allow the bombardment of a solid target capable of being used to produce the PET isotope copper-64. In order to have the maximum usefulness, the design needed to integrate many aspects of the current install base of cyclotrons and PET targets. Specifically it would need to interface and operate with the existing cooling system, control system and physical space.

The reaction rate of the nickel-64 (p,n) copper-64 reaction was studied to verify the production capability at 11 MeV. A one dimensional thermal approximation was used to identify critical material and geometric parameters that could be manipulated to increase performance. The approximation indicated that it would be feasible to operate within the existing parameters.

Based on the design specifications, a detailed design was completed and fabricated. In testing at maximum beam current, the target disk and seals showed no signs of surface damage while the high vacuum integrity was maintained. Utilizing the design retrofitted onto an existing cyclotron, useful quantities of copper-64 were produced in operational testing at a host facility.

The design was demonstrated to be capable of enabling a commercial or research institution to begin a development program with radiopharmaceuticals produced from copper-64 without sacrificing existing production or research. While the design has been utilized to produce copper-64, the operational functionality of the system allows for the production of other solid target isotopes with similar conditions.

An expansion of the thermal model could provide design guidance for future work related to increased beam current or geometric configurations. As the use of copper-64 related radiopharmaceuticals increases, the need to increase production beyond single dose levels will be necessary. Also, other solid target materials might be developed which are more sensitive to the affects of thermal stress. It would be interesting to study the affects of integrating the cooling path into the target disk. This might be accomplished by a series of external grooves or internal pathways.

In order to speed processing and reduce radiation exposure, mechanical automation of the loading step might prove to be beneficial as usage increases and multi-target disk production becomes standard practice.

References

1. Valk, Peter E. ,et al. Positron Emission Tomography : Basic Science and Clinical Practice, (2002) Springer, London.

2. Vallabhajosula, Shankar. Molecular Imaging : Radiopharmaceuticals for PET and SPECT, (2009) Springer, Berlin.

3. Marti, Felix. Cyclotrons and their Applications, Sixteenth International Conference, East Lansing Michigan, May 2001.

4. Smith, Suzanne V., Molecular Imaging with Copper-64. *Journal of Inorganic Biochemistry*, 98, (2004), 1874-1901.

5. McCarthy, Deborah W. Efficient Production of High Specific Activity 64Cu Using a Biomedical Cyclotron. *Nuclear Medicine and Biology*, Vol 24, pp 35-43, 1997.

6. Szelecsenyi F. Excitation Functions of proton-induced nuclear reactions on enriched nickel-61 and nickel-64. *Applied Radioactive Isotopes*, (1993), 575-580.

7. Saha, Gopal B. Basics of Pet Imaging : Physics, Chemistry and Regulations. Springer, (2005). Springer .Berlin.

8. Chadwick, M.B. Thick Target Neutron, g-Ray and Radionuclide Production for Protons below 12 MeV on Nickel and Carbon Beam Stops. *Proceedings of the American Nuclear Society Winter Meeting,* Albuquerque , 1997.

9. Welch, Michael J. Handbook of Radiopharmaceuticals : Radiochemistry and Applications, (2003). Wiley, New York.

10. Avila-Rodriguez, M.A. 3D Modeling and Simulation of the Thermal Performance of Solid Cyclotron Targets. *Proceedings of the COSMOL Conference*, Boston, 2007.

11. Avallone, Eugene A. Marks' Standard Handbook for Mechanical Engineers. (1987) Ninth Edition. McGraw-Hill Book Company, New York.

12. Schlyer, David J. Cyclotron Targetry for Production of short-Lived Positron Emitters. *Brookhaven National Lab publication,* BNL-43464, 1991.

13. Segre E. , Experimental Nuclear Physics, (1953) .Wiley, New York.

VITA

Andrew Williamson was born and raised in Huntsville Alabama. He graduated from the University of Tennessee with a Bachelor of Science degree in Mechanical Engineering. He is a registered Professional Engineer in the state of Tennessee. He has been employed by the Oak Ridge National Laboratory, Oak Ridge Tool-Engineering and Siemens Molecular Imaging. He is a former officer in the United States Naval Reserve.